

Chemical Vapor Deposition of Individual Single-Walled Carbon Nanotubes Using Nickel Sulfate as Catalyst Precursor

L. W. Liu,^{*,†,‡} J. H. Fang,[†] L. Lu,^{*,†} Y. J. Ma,[†] Z. Zhang,[†] H. F. Yang,[†] A. Z. Jin,[†] and C. Z. Gu[†]

Institute of Physics, Chinese Academy of Sciences, Beijing 100080, and Department of Physics, Qiqihar University, Qiqihar 161006, People's Republic of China

Received: May 26, 2004; In Final Form: August 13, 2004

Individual single-walled carbon nanotubes (SWNTs) were synthesized directly on a Si/SiO₂ substrate by chemical vapor deposition using methane as the feedstock and nickel sulfate as the catalyst precursor. This new surface growth approach yields SWNTs of diameter 0.7–3 nm and lengths of up to tens of micrometers. The SWNTs were characterized with scanning electron microscopy, atomic force microscopy, Raman spectroscopy, and electron transport measurements. Both metallic and semiconducting SWNTs were identified.

An individual single-walled carbon nanotube (SWNT) is considered to be an ideal one-dimensional system for fundamental studies. SWNTs are also promising building blocks for future nanoelectronic circuits. Primary progress has been achieved in the chemical vapor deposition (CVD) synthesis of SWNTs using iron-based catalysts. By utilizing Fe(NO₃)₃/Al₂O₃ or Fe/Mo bimetallic catalyst, high-quality individual SWNTs have been synthesized in the methane CVD approach.^{1,2} It has also been found that the Fe₂(SO₄)₃/Al₂O₃ catalyst produces a higher yield of SWNTs, and these are nearly free of graphitic particles in their more open textured structure compared to those produced with the Fe(NO₃)₃/Al₂O₃ catalyst.² In addition, selective growth of separate SWNTs has been achieved on an SiO₂ surface with a patterned iron salt catalyst via a CVD process with methane or a methane/hydrogen mixture as the feed gas.^{3,4} Nickel is another kind of catalyst successfully used in the bulk synthesis of SWNTs via laser ablation or arc discharge processes.^{5,6} An annealed nickel thin film is used in the CVD growth of multiwalled carbon nanotubes,^{7–9} and an ultrathin Ni/Al film is used in the CVD growth of individual SWNTs.¹⁰ However, compared with that of an iron salt solution, the use of a nickel salt solution as catalyst is so far not as successful in CVD synthesis of SWNTs. NiO catalyst decomposed from Ni(NO₃)₂ mainly produces defective multiwalled structures rather than individual SWNTs.¹ Nickel can also be formed by decomposition of nickel sulfate to nickel oxide and then by reduction of the latter. It would be interesting to investigate whether nickel generated in this way can be used to catalyze the growth of carbon nanotubes on a Si/SiO₂ surface. This is not obviously feasible since nickel sulfate is insoluble in many organic solvents but very soluble in water, while the Si/SiO₂ surface is normally hydrophobic. In this paper, we present a CVD method to grow individual SWNTs on a Si/SiO₂ surface by using nickel sulfate as the catalyst precursor, and using a methane and hydrogen mixture as the feed gas.

Silicon wafers with a 500 nm silicon dioxide layer (Si/SiO₂) are hydrophobic without treatment. We treated the surface with

oxygen plasma for 30 s at an oxygen gas flow rate of 40 sccm (standard cubic centimeter per minute) using Plasmalab 80 Plus. After the treatment, the surface of the wafer was strongly hydrophilic when dipped in deionized water. Nickel sulfate catalyst was prepared by sonication for 30 min of the solution composed of 2 mg of NiSO₄·6H₂O and 100 mL of deionized water. Then, the wafers were dipped in the solution for a few seconds. They were baked and placed in the center of a 1.5 in. diameter quartz tube in an electric tube furnace. After the tube was purged with argon gas at a flow rate of 5 L/min for 10 min, the flow rate was changed to 0.75 L/min and the furnace was heated from room temperature to 900 °C at a ramp rate of 5 °C/min. Then, we switched to hydrogen gas flow at a rate of 0.2 L/min for 1 h. CVD was carried out at 900 °C with a mixture of methane and hydrogen gases at flow rates of 1.5 and 0.1 L/min, respectively. The reaction time was 15 min. Finally, the furnace was cooled to room temperature with argon gas flowing at 0.5 L/min.

The scanning electron microscopy (SEM) images show that most of the carbon nanotubes possess a long and relatively straight structure (Figure 1a), indicating the absence of topological defects such as pentagons and heptagons. Some nanotubes are over 40 μm in length. When a few catalyst particles are not uniformly distributed, one can easily find in a catalyst-congregated area that some carbon nanotubes grow out from the catalyst particles (Figure 1b), suggesting a base-growth mechanism. Figure 2a shows the atomic force microscopy (AFM) tapping-mode image of the nanotubes within a 5 × 5 μm² scan field (with a Digital Instruments Nanoscope IIIa). The diameter of the carbon nanotubes can be determined from their topographic heights. Its distribution ranges from 0.7 to 3 nm, as shown in Figure 2b. The average diameter of the 35 carbon nanotubes measured is 1.59 nm. According to Kong and co-workers' investigation, nanotubes with a diameter of less than 2.5 nm are mostly (>90%) individual SWNTs.¹ We thus conclude that most of our carbon nanotubes are individual SWNTs.

The Raman spectrum (taken with a Renishaw RM1000 confocal micro-Raman spectrometer) also supports the above argument that our nanotubes are SWNTs. The wavelength of the excitation laser was 633 nm. The spectrum of the as-grown sample on the Si/SiO₂ substrate is shown in Figure 3 and is similar to a previously reported spectrum for isolated SWNTs.

* To whom correspondence should be addressed. E-mail: lilu@aphy.iphy.ac.cn.

[†] Chinese Academy of Sciences.

[‡] Qiqihar University.

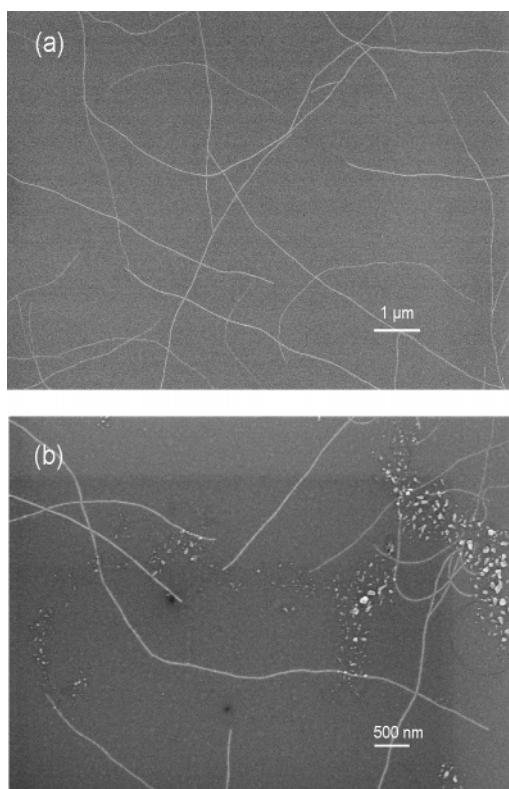


Figure 1. SEM images of carbon nanotubes grown on Si/SiO₂ substrates: (a) long and relatively straight carbon nanotubes; (b) SWNTs in an area of congregated catalyst particles.

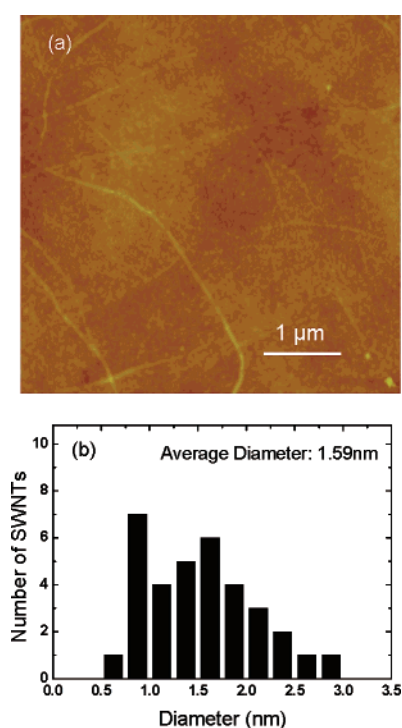


Figure 2. (a) AFM image of the carbon nanotubes grown on a Si/SiO₂ substrate. (b) Diameter distribution histogram of the nanotubes. The average diameter is 1.59 nm, taken from 35 observed samples.

Besides the Raman signals of the substrate at 303, 521, and 963 cm⁻¹,^{11,12} two peaks corresponding to the tangential vibrations of an SWNT (e.g., at 1591.9 and 1578.4 cm⁻¹ in Figure 3a) are always seen in different batches of samples. In addition, the weak radial breathing mode (RBM) at 185.4 cm⁻¹

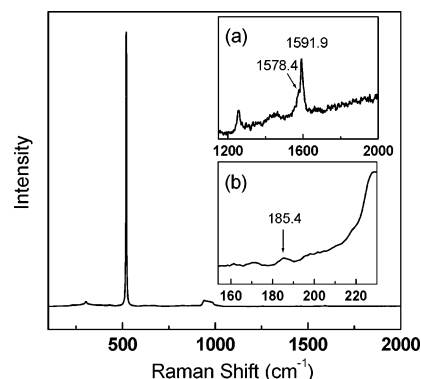


Figure 3. Raman spectrum of SWNTs on a Si/SiO₂ substrate. Peaks at 303, 521, and 963 cm⁻¹ come from the substrate. Inset a: Tangential vibration modes at 1591.9 and 1578.4 cm⁻¹. Inset b: Radial breathing mode of SWNTs at 185.4 cm⁻¹.

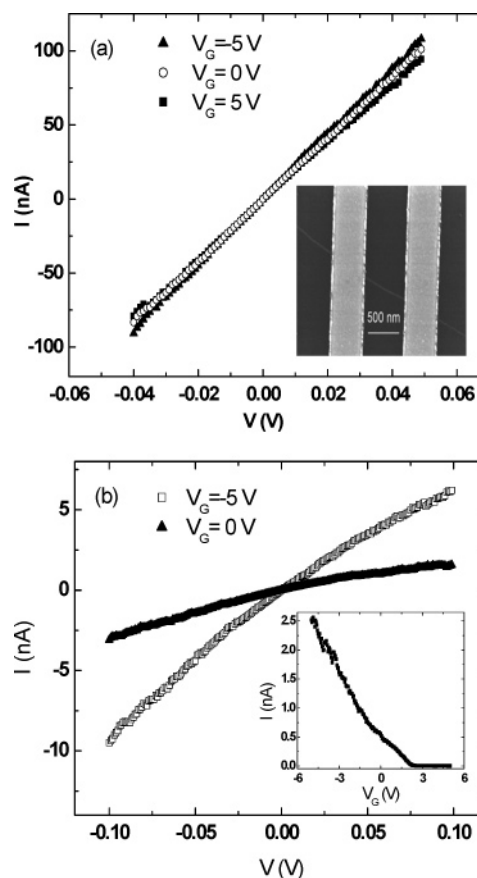


Figure 4. (a) *I*-*V* curves of a metallic SWNT at room temperature under different gate voltages. The inset shows an SEM image of an individual SWNT connected by two titanium-gold electrodes of 450 nm width and 60 nm thickness each, spaced by 650 nm. (b) Room-temperature *I*-*V* curves of a p-type semiconducting SWNT at 0 and -5 V gate voltages. The inset is the dependence of the current on the gate voltages under 20 mV bias voltage.

could also be identified in Figure 3b, though it is not as significant as in the resonant case of using 785 nm excitation, indicating a diameter $d_t = 1.33$ nm for the SWNTs according to the formula $\omega_{\text{RBM}} = 248/d_t$.¹²

Electrical contacts to the individual SWNT were fabricated by the standard lift-off technique using electron beam lithography (with a Raith 150); see the inset in Figure 4a. Titanium (10 nm thick) and gold (50 nm thick) were deposited as source and drain electrodes with widths of 450 nm and a spacing of 650 nm. The doped silicon substrate was used as the back gate.

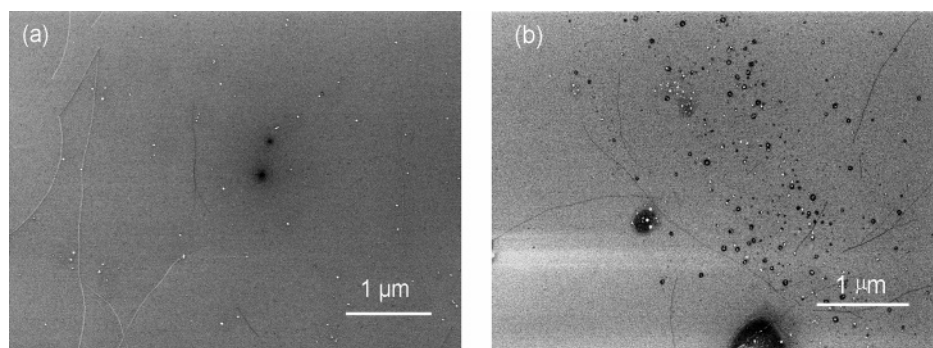


Figure 5. SEM images of carbon nanotube growth with (a) and without (b) hydrogen gas coflow. In the absence of hydrogen gas coflow, amorphous carbons are deposited at the catalyst particle sites in the form of balls.

At room temperature, the two-probe resistance of the as-grown samples ranges from a few hundred kilohms to a few hundred megaohms. Figure 4a shows the current–voltage (I – V) curves of a ~ 400 k Ω SWNT at various gate voltages. The linear behavior of the I – V curves and the absence of gate voltage dependence indicate that this is a metallic tube. Figure 4b shows an asymmetric and nonlinear I – V curve characteristic of a p-type semiconducting SWNT, also at room temperature. The two-probe resistance of this tube is around 40 M Ω at zero gate voltage. The inset shows the gate voltage dependence of the current under a bias voltage of 20 mV. The current can be turned off by applying a positive gate voltage of ~ 2 V.

We have also studied the effect of hydrogen gas flow in the CVD process. Figure 5 is a comparison between the results obtained with (0.05 L/min) and without hydrogen gas coflow, while keeping all other conditions unchanged. First, the probability of finding SWNTs on the substrate is very low if there is no hydrogen gas flow. Shown in Figure 5b is one of the very few places on the substrate that we can find SWNTs. Second, it can be seen that in the absence of hydrogen coflow there are amorphous carbon balls, instead of carbon nanotubes, growing at the sites of the catalyst particles, resulting in a low yield of SWNTs. On the contrary, adding hydrogen gas coflow during the CVD process seems to protect the catalyst from being poisoned by amorphous carbon deposits.

To conclude, we have succeeded in using nickel sulfate catalyst to grow individual SWNTs directly on a silicon substrate

via a CVD process, and such surface-grown materials facilitate the fabrication of nanodevices with no further treatment for purification and dispersion.

Acknowledgment. We thank Dr. W. Yi of Harvard University for his valuable discussions.

References and Notes

- (1) Kong, J.; Cassell, A. M.; Dai, H. *Chem. Phys. Lett.* **1998**, 292, 567.
- (2) Cassell, A. M.; Raymakers, J. A.; Kong, J.; Dai, H. *J. Phys. Chem. B* **1999**, 103, 6484.
- (3) Kong, J.; Soh, H. T.; Cassell, A. M.; Quate, C. F.; Dai, H. *Nature* **1998**, 395, 878.
- (4) Franklin, N. R.; Li, Y.; Chen, R. J.; Javey, A.; Dai, H. *Appl. Phys. Lett.* **2001**, 79, 4571.
- (5) Thess, A.; Lee, R.; Nikolaev, P.; Dai, H.; Petit, P.; Robert, J.; Xu, C.; Lee, Y. H.; Kim, S. G.; Rinzler, A. G.; Colbert, D. T.; Scuseria, G. E.; Tománek, D.; Fischer, J. E.; Smalley, R. E. *Science* **1996**, 273, 483.
- (6) Bethune, D. S.; Kiang, C. H.; de Vries, M. S.; Gorman, G.; Savoy, R.; Vazquez, J.; Beyers, R. *Nature* **1993**, 363, 605.
- (7) Ren, Z. F.; Huang, Z. P.; Xu, J. W.; Wang, J. H.; Bush, P.; Siegal, M. P.; Provencio, P. N. *Science* **1998**, 282, 1105.
- (8) Wei, B.; Zhang, Z. J.; Ramanath, G.; Ajayan, P. M. *Appl. Phys. Lett.* **2000**, 77, 2985.
- (9) Delzeit, L.; Nguyen, C. V.; Chen, B.; Stevens, R.; Cassell, A.; Han, J.; Meyyappan, M. *J. Phys. Chem. B* **2002**, 106, 5629.
- (10) Zhang, R. Y.; Amlani, I.; Baker, J.; Tresek, J.; Tsui, R. K.; Fejes, P. *Nano Lett.* **2003**, 3, 731.
- (11) Jorio, A.; Souza Filho, A. G.; Dresselhaus, G.; Dresselhaus, M. S.; Swan, A. K.; Ünlü, M. S.; Goldberg, B. B.; Pimenta, M. A.; Hafner, J. H.; Lieber, C. M.; Saito, R. *Phys. Rev. B* **2002**, 65, 155412.
- (12) Jorio, A.; Saito, R.; Hafner, J. H.; Lieber, C. M.; Hunter, M.; McClure, T.; Dresselhaus, G.; Dresselhaus, M. S. *Phys. Rev. Lett.* **2001**, 86, 1118.